

## LIQUID BRIDGE STABILITY DATA

I. MARTÍNEZ and J.M. PERALES

*Universidad Politécnica de Madrid, ETSI Aeronáuticos, 28040-Madrid, Spain*

Received 8 August 1985; manuscript received in final form 24 July 1986

High precision computations of the minimum volume and the corresponding shape of axisymmetric liquid bridges at rest, anchored to unequal and coaxial discs, are presented. The tables and graphs provide a standard for comparison of linearized and other approximate models, as well an aid in detecting very small departures in shape due to weak (for instance, electrostatic) forces. Relevance to crystal growth by the floating zone technique in the absence of gravity is elucidated.

### 1. Introduction

The configuration shown in fig. 1 is considered. This is a classical setup that has been used since the pioneering work of Plateau in the 19th century. Because in most cases the influence of the protruding solid tips immersed in the liquid is just a constant shift in the scale of volumes in tables and graphs, the solid/liquid interface is assumed to be planar.

The different shapes a liquid bridge can present and the criteria for their stability are well documented [1–5], but the direct problem of finding the shape for a given geometry ( $R_1$ ,  $R_2$  and  $L$ ) and volume ( $V$ ) is cumbersome in practice, and it is even more cumbersome to find the minimum volume for a given geometry, although helpful approximations are available [6].

It might be argued that time has passed for the publication of long data tables such as those following. Unfortunately, for the time being, computing the shape corresponding to a liquid bridge of say 10 and 20 mm in diameter, a distance of 30 mm apart, in the limiting configuration of minimum volume, may take several hours of cumbersome interaction at a computer desk after days of preparatory work, and this burden may be saved to the many crystal-growth investigators interested in floating zone stability.

Data are presented here in a very compact

form; all the information to describe a shape is reduced to three numbers. Thus, nearly 200, high precision, singular shapes are documented in this paper. The more complex problem of liquid bridges in a gravity field and/or with rotation has not, so far, been reduced in such a way, although some, low precision, graphical information is available [7–11].

The relevance of the data supplied here to crystal growth by the floating zone technique in the absence of gravity may be illustrated by the following example. In recent experiments involving the growth of a silicon rod in space [12,13], one of the two rods processed suffered a bridge disruption. Image recordings seem to indicate that a departure from expected equilibrium shapes already existed, but, how far from the expected

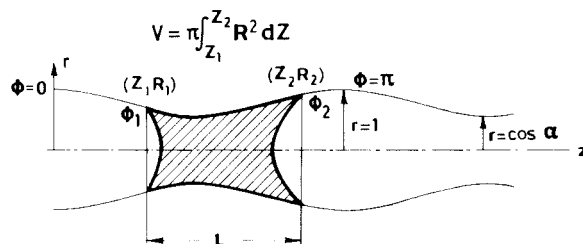


Fig. 1. Nomenclature for an anchored liquid bridge at rest, in absence of gravity, characterized by its geometry  $R_1$ ,  $R_2$  and  $L$ , and the straight cross-section volume  $V$  (liquid plus protruding tips, if any).

stability limit did the rupture occur? The collection of data supplied here could be of assistance not only for a posteriori analysis but also during actual growing. Moreover, because small disturbances upon the molten shape are so greatly amplified near the minimum volume stability limit, a fine comparison of actual and predicted shapes could give clues about surface tension gradients (predicted shapes assume constant surface tension), for instance, that may be difficult to detect otherwise (measuring surface temperatures, for instance).

## 2. Formulation

For a liquid bridge at rest, in the absence of gravity, surrounded by another fluid, with constant interface tension (constant free energy per unit area), the equilibrium shape is a surface of revolution of uniform mean curvature (local formulation) or, equivalently, a surface of revolution of minimum effective area (integral formulation). If the liquid is anchored to the disc edges, the effective area is just the liquid/fluid interface area. The actual meridian curve generating the surface of revolution must be a piece of an axially periodic Plateau curve: cylinder, unduloids, catenary, nodoids and sphere, all of which except the catenary can be expressed in parametric form in terms of the elliptic integrals of first (F) and second (E) class [4]:

$$z(\alpha, \phi) = \cos \alpha F(\alpha, \phi) + E(\alpha, \phi), \quad (1a)$$

$$r(\alpha, \phi) = (1 - \sin^2 \alpha \sin^2 \phi)^{1/2}, \quad (1b)$$

where  $\alpha$  identifies the Plateau curve ( $\cos \alpha$  is the ratio of hollow-to-summit radii, fig. 1) and  $\phi$  is a parameter that makes the curve being run. The actual shape would be delimited by knowing  $\alpha$  and the two extremes  $\phi_1$  and  $\phi_2$ ; in nondimensional terms, using  $(R_1 + R_2)/2$  as unit length,

$$Z(\alpha, \phi, \phi_1, \phi_2) = 2 \frac{z(\alpha, \phi) - z(\alpha, \phi_1)}{r(\alpha, \phi_1) + r(\alpha, \phi_2)}, \quad (2a)$$

$$R(\alpha, \phi, \phi_1, \phi_2) = 2 \frac{r(\alpha, \phi)}{r(\alpha, \phi_1) + r(\alpha, \phi_2)}, \quad (2b)$$

with  $\phi_1 < \phi < \phi_2$ . The algebraic relationship between the three internal parameters  $\alpha$ ,  $\phi_1$  and  $\phi_2$  and the physical (dimensional) input data  $R_1$ ,  $R_2$ ,  $L$  and  $V$  is:

$$K \equiv \frac{R_1}{R_2} = \frac{r(\alpha, \phi_1)}{r(\alpha, \phi_2)}, \quad (3a)$$

$$\Lambda \equiv \frac{L}{R_1 + R_2} = \frac{z(\alpha, \phi_2) - z(\alpha, \phi_1)}{r(\alpha, \phi_2) + r(\alpha, \phi_1)}, \quad (3b)$$

$$V \equiv \frac{8V}{(R_1 + R_2)^3} = \frac{8[v(\alpha, \phi_2) - v(\alpha, \phi_1)]}{[r(\alpha, \phi_2) + r(\alpha, \phi_1)]^3}, \quad (3c)$$

where, besides the functions  $z(\alpha, \phi)$  and  $r(\alpha, \phi)$  already introduced in eq. (1), the function  $v(\alpha, \phi)$  that gives the volume of the Plateau curve from  $\phi = 0$  up to section  $\phi$  is used [4]:

$$v(\alpha, \phi) = \frac{1}{3}\pi \left[ r\sqrt{(1-r^2)(r^2 - \cos^2 \alpha)} - z \cos \alpha + 2(1 + \cos \alpha)^2 E \right]. \quad (4)$$

The problem is to pass from the physical variables to the intrinsic shape values  $\alpha$ ,  $\phi_1$  and  $\phi_2$  by means of eqs. (3), but solving this system is not an easy task (see appendix 1) and for most applications with  $\Lambda - \pi \ll 1$ ,  $V - 2\pi\Lambda \ll 1$  and  $H \ll 1$  ( $H = (1 - K)/(1 + K)$  is used here instead of  $K$ ,  $K = (1 - H)/(1 + H)$  for convenience, and  $H \ll 1$  is equivalent to  $K - 1 \ll 1$ ), the direct linear approximation [6],

$$\begin{aligned} R^2(Z, H, \Lambda, V) &= 1 + \frac{V - 2\pi\Lambda}{2\pi\Lambda} \frac{\cos(Z - Z_1) - \cos \Lambda}{\sin \Lambda/\Lambda - \cos \Lambda} \\ &\quad + 2H \frac{\sin(Z - Z_1)}{\sin \Lambda} \\ &\quad + H^2 \frac{\sin \Lambda/\Lambda - \cos(Z - Z_1)}{\sin \Lambda/\Lambda - \cos \Lambda}, \end{aligned} \quad (5)$$

may be good enough.

### 2.1. Stability

Inversion of the system of eqs. (3) gives the parameters to easily compute the shape, with eqs.

(2), for a given geometry. To conduct a stability analysis, the zero-jacobian condition (differential approach, Martínez [1983]) or the conjugate point condition (variational approach, Gillette and Dyson [1971]) must be used. The limiting condition for stability, following the former method, is

$$J(\alpha, \phi_1, \phi_2) = \begin{vmatrix} \partial K/\partial\alpha & \partial\Lambda/\partial\alpha & \partial V/\partial\alpha \\ \partial K/\partial\phi_1 & \partial\Lambda/\partial\phi_1 & \partial V/\partial\phi_1 \\ \partial K/\partial\phi_2 & \partial\Lambda/\partial\phi_2 & \partial V/\partial\phi_2 \end{vmatrix} = 0. \quad (6)$$

For  $K$  and  $\Lambda$  fixed, the system formed by eqs. (3) and (6) consists of four equations with four unknowns,  $\alpha$ ,  $\phi_1$ ,  $\phi_2$  and  $V$ , which, if the appropriate solution is chosen (the equations are multivalued), give the minimum stable volume,  $V_{\min}$ . A linear approximation [4] may be used advantageously for long bridges between slightly different discs:

$$V_{\min} = 2\Lambda(2\Lambda - \pi) - 3\pi \left[ \frac{9}{2} \frac{H}{1 - \sin \Lambda/\Lambda} \right]^{2/3}. \quad (7)$$

2.2. Special cases

All curves and graphs presented in this paper correspond to points that are singular in the transformation  $K, \Lambda, V \leftrightarrow \alpha, \phi_1, \phi_2$  according to eq. (6), but we refer now to singularities that remain in the computation after eq. (6) is accounted for. They correspond to the catenoidal stability limit (already mentioned in section 1 when mentioning the catenary as a special meridian curve), to the stability limit with zero slope ( $dr/dz = 0$ ) at the larger disc, and to the stability limit of minimum Plateau undulation (minium  $|\alpha|$  for all  $V_{\min}$  at constant  $K$ ; see table 1).

Table 1 gives  $V_{\min}$  versus  $\Lambda$  for various disc ratios  $K$ , and the internal parameters to compute the actual shape by eq. (2), as explained in appendix 3.

2.2.1. Catenoidal limit

For every disc ratio  $K$ , there is one series of shapes not dealt with in eq. (1) because it becomes singular for  $\alpha = \pi/2$  that would correspond to

that series. Although they might be approached asymptotically, their importance deserves a special analysis. These shapes are catenoidal, that is, portions of  $r = \cosh z$  with the appropriate scaling. One of these equilibrium catenoids lies on the minimum volume limit and thus must be found

Table 1  
Nondimensional minimum volume  $V$ , for liquid bridges at rest, anchored to the edges of coaxial discs of radius  $R_1$  and  $R_2$ , as a function of nondimensional disc separation  $\Lambda$ , and diameter ratio  $K$ ; the parameters  $\alpha$  and  $\phi_1$  serve to compute the interface shape (appendix 3); the liquid/solid angle at both ends,  $\theta_1$  and  $\theta_2$  is also presented to check for limiting contact angle conditions.

$\Lambda$	$V$	$\alpha$	$\phi_1$	$\theta_1$	$\theta_2$
$K = 1$					
0.6	1.107	-1.5231	1.3502	24.7	24.7
0.8	1.744	-1.4567	1.0526	41.0	41.0
1.0	2.431	-1.3978	0.8061	54.0	54.0
1.2	3.187	-1.3447	0.6018	64.3	64.3
1.4	4.025	-1.2959	0.4316	72.4	72.4
1.6	4.955	-1.2504	0.2882	78.8	78.8
1.8	5.984	-1.2075	0.1660	83.9	83.9
2.0	7.118	-1.1664	0.0605	87.9	87.9
2.2	8.372	-1.1002	0.0000	90.0	90.0
2.4	9.915	-0.9770	0.0000	90.0	90.0
2.6	11.855	-0.8346	0.0000	90.0	90.0
2.8	14.270	-0.6620	0.0000	90.0	90.0
3.0	17.245	-0.4253	0.0000	90.0	90.0
3.2	20.871	-0.2692	1.5708	90.0	90.0
3.4	25.247	-0.5427	1.5708	90.0	90.0
3.6	30.477	-0.6948	1.5708	90.0	90.0
3.8	36.669	-0.8025	1.5708	90.0	90.0
4.0	43.937	-0.8851	1.5708	90.0	90.0
$K = 0.9$					
0.6	1.115	-1.5235	1.3667	24.6	24.6
0.8	1.762	-1.4567	1.0903	39.9	41.8
1.0	2.462	-1.3970	0.8691	51.8	55.6
1.2	3.240	-1.3420	0.6993	60.7	66.8
1.4	4.119	-1.2885	0.5799	67.1	75.8
1.6	5.131	-1.2322	0.5124	71.2	83.0
1.8	6.328	-1.1689	0.4950	73.6	88.6
2.0	7.778	-1.0985	0.5188	74.8	92.7
2.2	9.557	-1.0263	0.5763	75.6	95.9
2.4	11.749	-0.9608	0.6649	76.1	98.3
2.6	14.440	-0.9129	0.7807	76.5	100.3
2.8	17.724	-0.8920	0.9113	76.8	101.9
3.0	21.698	-0.8990	1.0366	77.1	103.3
3.2	26.466	-0.9260	1.1420	77.3	104.4
3.4	32.136	-0.9630	1.2239	77.5	105.4
3.6	38.823	-1.0029	1.2857	77.7	106.2
3.8	46.646	-1.0418	1.3323	77.9	107.0

Table 1 (continued)

$\Lambda$	$V$	$\alpha$	$\phi_1$	$\theta_1$	$\theta_2$
<i>K</i> = 0.8					
0.6	1.142	-1.5251	1.3921	24.4	24.2
0.8	1.821	-1.4568	1.1417	38.5	42.2
1.0	2.564	-1.3951	0.9510	49.3	56.7
1.2	3.408	-1.3365	0.8177	57.1	68.2
1.4	4.391	-1.2780	0.7383	62.4	77.4
1.6	5.566	-1.2178	0.7066	66.0	84.7
1.8	6.994	-1.1569	0.7147	68.3	90.4
2.0	8.748	-1.0988	0.7553	69.9	95.0
2.2	10.910	-1.0500	0.8220	71.1	98.6
2.4	13.566	-1.0165	0.9071	72.0	101.6
2.6	16.810	-1.0019	1.0001	72.7	104.1
2.8	20.742	-1.0054	1.0901	73.3	106.1
3.0	25.468	-1.0224	1.1693	73.8	107.9
3.2	31.097	-1.0474	1.2348	74.3	109.5
3.4	37.748	-1.0760	1.2876	74.7	110.8
3.6	45.540	-1.1052	1.3295	75.1	112.0
<i>K</i> = 0.7					
0.6	1.194	-1.5277	1.4235	24.6	23.5
0.8	1.931	-1.4573	1.2019	37.5	42.2
1.0	2.752	-1.3932	1.0411	47.1	57.1
1.2	3.701	-1.3323	0.9373	54.1	69.0
1.4	4.834	-1.2731	0.8836	59.0	78.5
1.6	6.212	-1.2161	0.8713	62.5	86.0
1.8	7.906	-1.1645	0.8924	65.0	92.1
2.0	9.996	-1.1223	0.9387	66.8	97.0
2.2	12.570	-1.0936	1.0018	68.3	101.0
2.4	15.723	-1.0803	1.0725	69.4	104.4
2.6	19.556	-1.0811	1.1425	70.4	107.3
2.8	24.178	-1.0928	1.2059	71.2	109.7
3.0	29.700	-1.1113	1.2602	71.9	111.8
3.2	36.243	-1.1335	1.3053	72.5	113.6
3.4	43.930	-1.1570	1.3422	73.0	115.2
<i>K</i> = 0.6					
0.6	1.278	-1.5307	1.4551	25.7	22.7
0.8	2.108	-1.4581	1.2642	37.1	42.0
1.0	3.043	-1.3926	1.1314	45.8	57.4
1.2	4.142	-1.3317	1.0517	52.3	69.6
1.4	5.470	-1.2757	1.0169	56.9	79.4
1.6	7.101	-1.2265	1.0177	60.4	87.3
1.8	9.114	-1.1872	1.0452	62.9	93.8
2.0	11.600	-1.1605	1.0901	65.0	99.1
2.2	14.655	-1.1472	1.1436	66.6	103.5
2.4	18.384	-1.1461	1.1984	67.9	107.2
2.6	22.895	-1.1543	1.2493	69.0	110.4
2.8	28.307	-1.1686	1.2941	69.9	113.1
3.0	34.740	-1.1864	1.3321	70.7	115.4
3.2	42.323	-1.2056	1.3638	71.4	117.5

Table 1 (continued)

$\Lambda$	$V$	$\alpha$	$\phi_1$	$\theta_1$	$\theta_2$
<i>K</i> = 0.5					
0.6	1.408	-1.5327	1.4808	28.1	22.1
0.8	2.374	-1.4591	1.3233	38.0	42.0
1.0	3.471	-1.3940	1.2180	45.7	57.8
1.2	4.772	-1.3364	1.1601	51.6	70.5
1.4	6.357	-1.2874	1.1409	56.0	80.7
1.6	8.311	-1.2493	1.1503	59.3	89.0
1.8	10.725	-1.2232	1.1790	62.0	95.7
2.0	13.700	-1.2098	1.2177	64.0	101.4
2.2	17.345	-1.2073	1.2593	65.7	106.1
2.4	21.772	-1.2131	1.2993	67.1	110.1
2.6	27.104	-1.2244	1.3351	68.2	113.5
2.8	33.467	-1.2388	1.3660	69.2	116.4
3.0	40.992	-1.2547	1.3921	70.1	119.0
<i>K</i> = 0.4					
0.6	1.616	-1.5314	1.4970	32.3	22.5
0.8	2.775	-1.4599	1.3765	40.5	42.7
1.0	4.098	-1.3989	1.3000	47.1	58.9
1.2	5.677	-1.3488	1.2631	52.3	72.0
1.4	7.607	-1.3107	1.2566	56.4	82.5
1.6	9.987	-1.2856	1.2702	59.5	91.1
1.8	12.923	-1.2719	1.2958	62.0	98.2
2.0	16.530	-1.2686	1.3254	64.0	104.0
2.2	20.928	-1.2727	1.3550	65.6	109.0
2.4	26.245	-1.2816	1.3821	67.0	113.2
2.6	32.612	-1.2933	1.4059	68.2	116.8
2.8	40.168	-1.3063	1.4262	69.2	119.9
<i>K</i> = 0.3					
0.6	1.976	-1.5252	1.5057	38.7	24.7
0.8	3.405	-1.4617	1.4254	45.0	44.9
1.0	5.048	-1.4108	1.3786	50.3	61.3
1.2	7.019	-1.3732	1.3607	54.7	74.5
1.4	9.430	-1.3489	1.3628	58.1	85.2
1.6	12.398	-1.3362	1.3765	60.9	94.0
1.8	16.047	-1.3327	1.3953	63.1	101.3
2.0	20.509	-1.3357	1.4151	64.9	107.3
2.2	25.919	-1.3427	1.4337	66.5	112.4
2.4	32.418	-1.3520	1.4502	67.7	116.8
2.6	40.154	-1.3623	1.4645	68.8	120.5
<i>K</i> = 0.2					
0.6	2.656	-1.5170	1.5155	47.3	29.9
0.8	4.475	-1.4703	1.4748	51.7	49.5
1.0	6.592	-1.4367	1.4548	55.6	65.6
1.2	9.142	-1.4157	1.4505	58.9	78.8
1.4	11.852	-1.4063	1.4544	61.1	88.3
1.6	16.092	-1.4025	1.4653	63.7	98.2
1.8	20.777	-1.4047	1.4762	65.6	105.5
2.0	26.467	-1.4100	1.4869	67.1	111.6
2.2	33.318	-1.4169	1.4965	68.4	116.7
2.4	41.488	-1.4244	1.5049	69.4	121.1

Table 1 (continued)

$\Lambda$	$V$	$\alpha$	$\phi_1$	$\theta_1$	$\theta_2$
$K = 0.1$					
0.6	4.105	-1.5214	1.5386	58.7	39.9
0.8	6.536	-1.5002	1.5279	61.1	58.3
1.0	9.416	-1.4876	1.5244	63.4	73.5
1.2	12.910	-1.4819	1.5252	65.4	86.0
1.4	17.182	-1.4808	1.5284	67.2	96.2
1.6	22.400	-1.4825	1.5324	68.6	104.6
1.8	28.737	-1.4857	1.5363	69.9	111.6
2.0	36.365	-1.4897	1.5400	70.9	117.4
2.2	45.462	-1.4939	1.5432	71.8	122.3

separately (for every disc ratio  $K$ ) as presented in table 2.

This limiting case has already had direct application in the study of disjoining pressure effects on thin liquid films on a solid surface [14], due to its relevance as the most sensitive liquid bridge configurations (the pressure jump across the interface is zero). Exact knowledge of these shapes is required to evaluate their effect when very small forces show up [14], so that, although the computations in this case are not so involved as in the other cases, the explicit form of the determinant corresponding to eq. (6) is presented in appendix 2.

2.2.2. Stability limit with cylindrical ending ( $dr/dz = 0$ ) at the larger disc

This is really a simplification with respect to

Table 2

Catenoidal stability limit; for every disc ratio  $K$ , a separation exists, such as the minimum stable volume  $V_{min}$  is a catenoidal shape stretching from  $z_1$  to  $z_2$  when scaled with the neck radius (that is,  $r = \cosh z$ );  $\theta_1$  and  $\theta_2$  are the angles the liquid forms with the discs; these points correspond to curve C in fig. 2

$K$	$z_1$	$z_2$	$\Lambda$	$V$	$\theta_1$	$\theta_2$
1.0	-2.2392	2.2392	0.4718	0.7129	12.2	12.2
0.9	-2.1745	2.2823	0.4738	0.7218	13.0	11.7
0.8	-2.0791	2.3079	0.4801	0.7517	14.3	11.4
0.7	-1.9501	2.3172	0.4900	0.8058	16.2	11.3
0.6	-1.7893	2.3180	0.5007	0.8842	19.0	11.2
0.5	-1.6015	2.3250	0.5071	0.9801	22.8	11.2
0.4	-1.3926	2.3599	0.5017	1.0761	27.9	10.8
0.3	-1.1658	2.4552	0.4747	1.1354	34.6	9.8
0.2	-0.9201	2.6721	0.4118	1.0878	43.5	7.9
0.1	-0.6433	3.1881	0.2869	0.7996	55.5	4.7

the general case in eq. (6), and is analyzed apart because of the following peculiar property [11]: it splits the minimum volume curve (for constant  $K$ ) in two regions, such as for longer bridges the neck travels towards the larger disc during the breaking process, whereas it narrows without axial shifting for shorter bridges. In this case

$$\phi_2 = \pi, \tag{8a}$$

$$\phi_1 = -\arcsin(\sqrt{1 - K^2} / \sin \alpha), \tag{8b}$$

$$J(\alpha, \phi_1, \phi_2) = J(\alpha) = 0. \tag{8c}$$

Results are shown in table 3. For the special case of equal discs ( $K = 1$ ), eq. (8c) reduces to  $2E(\alpha, \pi/2) - F(\alpha, \pi/2) = 0$ , which gives  $\Lambda = 2.128392$ , an important value that has appeared with different degrees of error in the literature.

2.2.3. Stability limit with minimum undulation

As mentioned above, the equilibrium shape of an axisymmetric liquid bridge in zero gravity corresponds to a piece of an axially periodic curve (Plateau curve) that can be identified by the hollow/summit radii ratio ( $\cos \alpha$ ), as shown in fig. 1. For every disc ratio  $K$ , there is a minimum volume stability limit with a minimum value of  $|\alpha|$ ; it has been asymptotically approached numerically by reducing  $|\alpha|$  when solving eq. (6), and the results are presented in table 4.

Table 3

Minimum volume shape with cylindrical ending ( $dr/dz = 0$ ) at the larger disc; for every disc ratio  $K$ , the separation  $\Lambda$  and the corresponding volume  $V_{min}$  are given; with  $K$ ,  $\alpha$  and  $\phi_1$ , the actual shape may be computed as explained in appendix 3. these points correspond to curve B in fig. 2

$K$	$\alpha$	$\phi_1$	$\Lambda$	$V$	$\theta_1$	$\theta_2$
1.0	-1.1407	0.0000	2.1283	7.901	90.0	90.0
0.9	-1.1476	0.4984	1.8620	6.748	74.0	90.0
0.8	-1.1618	0.7128	1.7832	6.862	68.1	90.0
0.7	-1.1825	0.8813	1.7270	7.246	64.2	90.0
0.6	-1.2099	1.0257	1.6778	7.834	61.4	90.0
0.5	-1.2447	1.1535	1.6284	8.623	59.8	90.0
0.4	-1.2880	1.2677	1.5726	9.630	59.1	90.0
0.3	-1.3410	1.3689	1.5036	10.890	59.6	90.0
0.2	-1.4049	1.4561	1.4111	12.454	61.7	90.0
0.1	-1.4810	1.5264	1.2739	14.389	66.2	90.0

Table 4

Minimum volume corresponding to minimum undulation ( $|\alpha|$  minimum); for every  $K$  there is a minimum  $|\alpha|$  versus  $\Lambda$  (see table 1) and it is presented here; these points correspond to curve A in fig. 2

$K$	$\alpha$	$\phi_1$	$\Lambda$	$V$	$\theta_1$	$\theta_2$
1.0	0.0000	0.0000	3.1416	19.739	90.0	90.0
0.9	-0.8913	0.9407	2.8451	18.556	76.9	102.2
0.8	-1.0012	1.0261	2.6561	17.839	72.9	104.7
0.7	-1.0790	1.1028	2.4851	17.265	69.9	105.7
0.6	-1.1452	1.1763	2.3185	16.777	67.4	105.8
0.5	-1.2070	1.2492	2.1513	16.389	65.3	105.0
0.4	-1.2685	1.3221	1.9778	16.093	63.8	103.4
0.3	-1.3327	1.3948	1.7949	15.944	63.1	101.1
0.2	-1.4025	1.4650	1.5945	15.975	63.7	98.0
0.1	-1.4808	1.5280	1.3801	16.717	67.0	95.3

### 3. Results and conclusions

The minimum volume for stability, versus bridge length, is presented in fig. 2 for several disc ratios  $K$ . The special cases described above have been explicitly included. High precision values can be found in the tables. The method to compute the limiting shapes for the points included, as well as how to extend the tables here given, are presented in appendix 3.

As an example, let us consider the bridges that can be formed between discs of  $R_1 = 10$  mm and  $R_2 = 20$  mm in diameter ( $R_1/R_2 = 0.5$ ), assuming a certain liquid having some  $30^\circ$  contact angle with the solid discs in the presence of the outer fluid. A short liquid bridge of  $L = 9$  mm in length ( $\Lambda = 0.6$ ) can easily be established by putting  $V = 1.5$  cm<sup>3</sup> ( $V = 3.6$ ) of liquid in between (fig. 3a). If the liquid is now gently withdraw at constant disc separation, the liquid border will detach from the disc edge when the angle at the edge of the larger disc diminishes to  $30^\circ$  (fig. 3b), well before the minimum volume  $V = 1.4$  given in table 1 is reached (fig. 3c).

Assume now that one manages to have a long liquid bridge of 30 mm ( $\Lambda = 2$ ) containing 9 cm<sup>3</sup> of liquid ( $V = 21.3$ , fig. 3d); when will such a bridge break if stretched at constant volume? (fig. 3f), or, alternatively, when will it break if liquid is removed at constant disc separation? (fig. 3e). Answers to these and similar questions are now

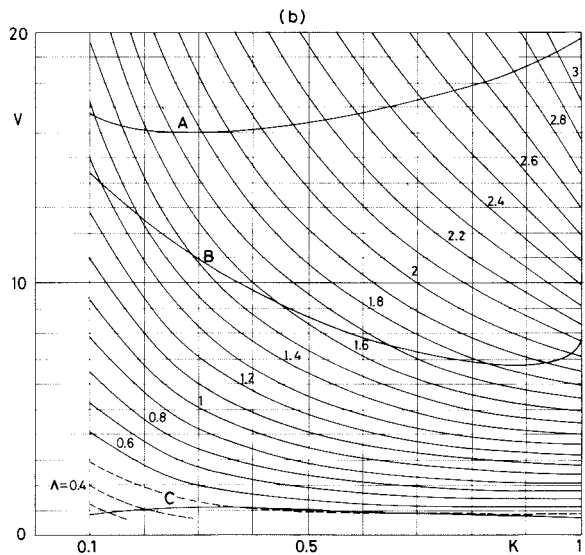
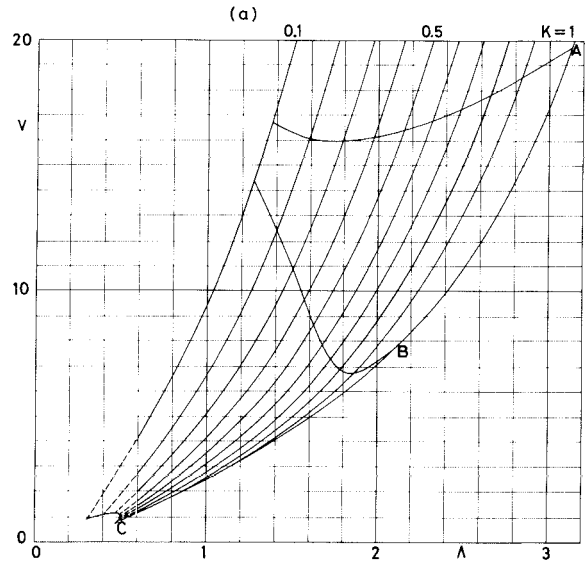


Fig. 2. Minimum volume  $V_{\min}$  for a liquid bridge anchored to coaxial discs of radii  $R_1$  and  $R_2$  a distance  $L$  apart. For every  $K = R_1/R_2$  there are three special points in the  $V_{\min}$  (A) curve: (A) bridge of minimum undulation; (B) bridge of  $dr/dz = 0$  (cylindrical ending) at the larger disc; (C) catenoidal bridge. (a)  $V_{\min}(\Lambda)$  for constant  $K$ ; (b)  $V_{\min}(K)$  for constant  $\Lambda$ .

easily obtained from table 1 (or fig. 2). For  $K = 0.5$  and  $V = 21.3$  we see in table 1 that  $\Lambda_{\max} \approx 2.4$  (36 mm long), whereas for  $K = 0.5$  and  $\Lambda = 2$  the minimum volume is  $V = 13.7$  (5.8 cm<sup>3</sup>). In both cases,  $\theta_2$  being greater than  $90^\circ$ , the breaking

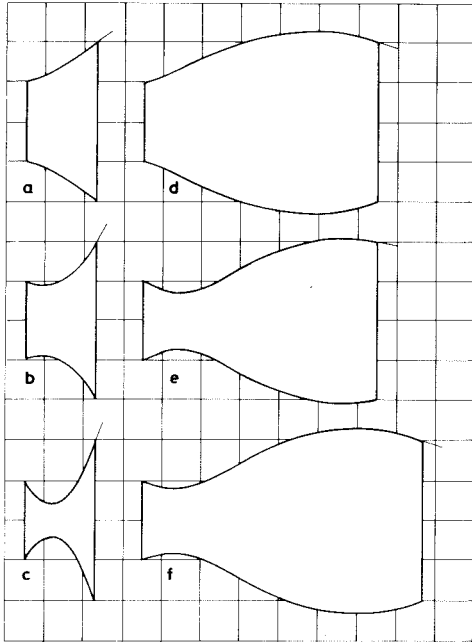


Fig. 3. Example of liquid bridge shapes for  $R_1=10$  mm,  $R_2=20$  mm. (a) Stable bridge with  $\Lambda=0.6$  and  $V=3.6$ , computed with eq. (9). (b) While removing liquid from the (a) shape, the liquid would recede from the disc edge if the liquid/solid limiting contact angle is assumed to be  $30^\circ$  (see section 3). (c) Minimum volume stability limit for  $K=0.5$  and  $\Lambda=0.6$ , computed as explained in appendix 3. (d) Stable bridge with  $\Lambda=2$  and  $V=21.3$ , computed with eq. (9). (e) Minimum volume stability limit for  $K=0.5$  and  $\Lambda=2$ , computed as explained in appendix 3. (f) Stability limit when stretching from (d) at constant volume.

shape (readily obtained from  $K$ ,  $\alpha$  and  $\phi_1$ ) will have a hollow and a summit.

As regarding the relevance of this results to the real floating zone problem, it might be argued that true molten zones do not have fixed volume or length as the model assumes, but the mechanical stability of a real floating zone (be it a melt or a solution) happens to have a much smaller characteristic time scale that thermal or physico-chemical instabilities and thus, for small time intervals, it is at all licit to treat the liquid volume and length as constants, as has already been successfully made in [15], where this same liquid-bridge model has been used to predict, with high accuracy, the outer-shape evolution (stable and unstable) of a real floating zone of molten silicon aboard an orbiting laboratory.

In conclusion, this paper presents (as far as we know for the first time) a comprehensive and highly compact data set on the minimum stable volume for liquid bridges between non-equal discs in absence of gravity; and not only the value of  $V_{\min}$  is given, but data necessary to compute the actual shape of the free surface in this limiting configuration is provided.

#### Appendix I. Shape computation for given $K$ , $\Lambda$ and $V$

Several methods have been investigated to compute the shape from primary data  $K$ ,  $\Lambda$  and  $V$ . In all cases, the problem being highly nonlinear, a fairly good initial guess is required; eq. (5) is an evaluable help in that respect.

If an algebraic solution of eq. (3) is desired, we recommend the specification of  $\alpha$  and computation  $\phi_1$  and  $\phi_2$  from the first two conditions in eq. (3); the first one may be solved explicitly as  $\phi_2 = \phi_2(K, \alpha, \phi_1)$  and the second one  $\Lambda(\alpha, \phi_1, \phi_2) = \Lambda$  by a standard root finder, thus obtaining a  $V = V(\alpha)$  relationship.

Another approach is by a series expansion in terms of orthogonal polynomials, for instance Tschebyscheff economization series. Thence, using  $L/2$  as unit length, the shape  $r = r(z)$  can be written as

$$r(z) = \sum_{n=0}^N a_n T_n(z),$$

with  $T_n$  the  $n$ th order Tschebyscheff polynomial, where the  $N+1$  coefficients  $a_n$  are to be found from the conditions  $r(-1) = R_1/L$ ,  $r(+1) = R_2/L$ ,

$$\int_{-1}^1 r^2 dz = \frac{V}{\pi L^3}$$

and

$$\int_{-1}^1 r \sqrt{1 + (dr/dz)^2} dz = \text{minimum}$$

for every possible variation of the coefficients. If the series is truncated at  $N=3$ ,  $a_0$ ,  $a_1$  and  $a_2$  can be explicitly solved for and the minimum of the

last integral with  $a_3$  easily found. Unfortunately this expedient procedure gives an accuracy of the same order as the straightforward expression of eq. (5).

As another approach, a very accurate solution can be found by direct integration of the differential equations for constant mean curvature (Laplace capillary equation) in the form

$$\frac{dr}{dz} = t \quad \text{with} \quad r|_{z=0} = 1 - H \tag{9a}$$

$$\frac{dt}{dz} = \frac{1+t^2}{r} - p(1+t^2)^{3/2} \quad \text{with} \quad t|_{z=0} = t_0, \tag{9b}$$

$$\frac{dv}{dz} = \pi r^2 \quad \text{with} \quad v|_{z=0} = 0, \tag{9c}$$

where the internal variable  $t$  (the local slope of the shape) and the nondimensional pressure jump across the free surface  $p$  (constant) are introduced. In this scheme  $H$ ,  $H = (1 - K)/(1 + K)$ , is given, and  $p$  and  $t_0$  are estimated with the aid of eq. (5). A standard Runge–Kutta numerical integration of eq. (9) from  $z = 0$  to  $z = 2\Lambda$  ( $\Lambda$  is given) then yields new values for  $H$  and  $V$

$$H = r|_{z=2\Lambda} - 1, \tag{10a}$$

$$V = \frac{8v|_{z=2\Lambda}}{(1 - H + r|_{z=2\Lambda})^3}, \tag{10b}$$

and a standard Newton–Raphson iteration is used to approach the specified  $H$  and  $V$  to the desired accuracy. The procedure, of course, becomes singular near the stability limit.

**Appendix 2. Stability limit corresponding to a catenoid**

Quasi-catenoidal shapes can be expressed, when properly scaled, as

$$r(z) = \cosh z + \epsilon y(z), \tag{11}$$

where  $\epsilon$  is a small number. After substitution in the equilibrium equation (Laplace capillary equation, or Euler–Lagrange equation in the variational formulation) the resulting stability equation

$$\frac{d^2y}{dz^2} - 2 \tanh z \frac{dy}{dz} + p \cosh^3 z = 0, \tag{12}$$

where  $p$  is an internal constant that, in addition to the two boundary conditions in eq. (12), is to be found from the three conditions

$$y(z_1) = 0, \tag{13a}$$

$$y(z_2) = 0, \tag{13b}$$

$$\int_{z_1}^{z_2} y(z) \cosh z \, dz = 0, \tag{13c}$$

which, upon substitution of the general solution of eq. (12) takes the form

$$\begin{vmatrix} \sinh z_1 & z_1 \sinh z_1 & \cosh^3 z_1 \\ & -\cosh z_1 & \\ \sinh z_2 & z_2 \sinh z_2 & \cosh^3 z_2 \\ & -\cosh z_2 & \\ (\cosh 2z_2 & f(z_2) - f(z_1) & g(z_2) - g(z_1) \\ -\cosh 2z_1)/4 & & \end{vmatrix} = 0, \tag{14}$$

where the functions  $f(z)$  and  $g(z)$  are

$$f(z) = -\frac{z}{2} - \frac{3}{8} \sinh(2z) + \frac{z}{4} \cosh(2z), \tag{15a}$$

$$g(z) = \frac{3z}{8} + \frac{1}{4} \sinh(2z) + \frac{1}{32} \sinh(4z). \tag{15b}$$

After substitution in eqs. (14) and (15) of

$$z_2 = \arg \cosh \frac{\cosh z_1}{K}, \tag{16}$$

the only remaining unknown is  $z_1$ , which is to be found from a nontrivial solution of eq. (14). After  $z_1$  is found the nondimensional bridge length and liquid volume are given by

$$\Lambda = \frac{z_2 - z_1}{\cosh z_2 + \cosh z_1}, \tag{17a}$$

$$V = 2 \frac{\sinh(2z_2) + 2z_2 - \sinh(2z_1) - 2z_1}{(\cosh z_2 + \cosh z_1)^3}. \tag{17b}$$

These values can be found in table 2 as a function of disc ratio  $K$ .

**Appendix 3. Summary of computational procedures**

*How to find the shape for points in tables 1, 3 and 4*

- (1) Given  $K$ ,  $\alpha$  and  $\phi_1$ .
- (2) Compute  $\phi_2 = \phi_2(K, \alpha, \phi_1)$  from eq. (3a); function  $\phi_2$  below.

(3) Compute the shape  $z = z(\alpha, \phi, \phi_1, \phi_2, r = r(\alpha, \phi, \phi_1, \phi_2))$ ; PROCEDURE Shape below.

*How to find new points*

(1) Given  $K$  and  $\Lambda$ .  
 (2) Compute  $\Lambda_B(K)$  from eq. (7) or points in curve B, fig. 2.

(3) Interpolate  $\alpha(K, \Lambda)$  from table 1.

(4) Compute  $\phi_1 = \phi_1(K, \Lambda, \alpha)$  from eq. (3b); function  $\phi_1$  below.

(5) Compute  $V_{\min}$  with eqs. (3c) and (4) and the shape  $(z, r)$  as above.

(6) To check or enhance accuracy, evaluate the jacobian in eq. (6), slightly change  $\alpha$ , and repeat steps 4 to 6.

*Pseudocode for the computer routines mentioned above*

FUNCTION  $r(\alpha, \phi)$

$$r = (1 - \sin^2 \alpha \sin^2 \phi)^{1/2}$$

FUNCTION  $\phi_2(K, \alpha, \phi_1)$

$$\phi_2 = \pi \pm \arcsin \frac{\sqrt{1 - (r(\alpha, \phi_1)/K)^2}}{\sin \alpha}$$

! use + if  $\Lambda < \Lambda_B$  or - if  $\Lambda > \Lambda_B$

PROCEDURE Shape( $\alpha, \phi_1, \phi_2, z, r, n$ )

!  $z$  &  $r$  are vectors of size  $n$

```
for i=0 to n
   $\phi = \phi_1 + (\phi_2 - \phi_1)(i/n)$ 
  Plateau( $\alpha, \phi, z(i), r(i)$ )
next i
```

FUNCTION  $\phi_1(K, \Lambda, \alpha)$

! always  $0 < \phi < \pi/2$

$$\phi_1 = \arcsin \frac{\sqrt{1 - K^2}}{\sin \alpha}$$

loop

```
 $\phi_2 = \phi_2(K, \alpha, \phi_1)$ 
Plateau( $\alpha, \phi_1, z_1, r_1$ )
Plateau( $\alpha, \phi_2, z_2, r_2$ )
New $\Lambda = (z_2 - z_1) / (r_2 + r_1)$ 
repeat loop, changing  $\phi_1$ , until New $\Lambda = \Lambda$ 
```

PROCEDURE Plateau( $\alpha, \phi, z, r$ )

```
Elliptic_integrals( $\alpha, \phi, F, E$ )
 $z = \cos \alpha F + E$ 
 $r = r(\alpha, \phi)$ 
```

! standard library routine

**References**

- [1] R.D. Gillette and D.C. Dyson, *Chem. Eng. J.* 3 (1972) 196.
- [2] S.R. Coriell and M.R. Cordes, *J. Crystal Growth* 42 (1977) 466.
- [3] A. Sanz and I. Martínez, *J. Colloid Interface Sci.* 93 (1983) 235.
- [4] I. Martínez, in: *Material Sciences under Microgravity*, ESA SP-191 (ESA, Paris, 1983) pp. 267–273.
- [5] J. Meseguer, *J. Crystal Growth* 67 (1984) 141.
- [6] J. Meseguer, in: *Material Sciences under Microgravity*, ESA SP-222 (ESA, Paris, 1984) pp. 297–300.
- [7] S.R. Coriell, S.C. Hardy and M.R. Cordes, *J. Colloid Interface Sci.* 60 (1977) 126.
- [8] E.A. Boucher and M.J.B. Evans, *J. Colloid Interface Sci.* 75 (1980) 409.
- [9] R.A. Brown and L.E. Scriven, *Phil. Trans. Roy. Soc. London A297* (1980) 51.
- [10] L.H. Ungar and R.A. Brown, *Phil. Trans. Roy. Soc. London A306* (1982) 347.
- [11] J. Meseguer and A. Sanz, *J. Fluid Mech.* 153 (1985) 83.
- [12] A. Eyer, B.O. Kolbesen and R. Nitsche, *J. Crystal Growth* 57 (1982) 145.
- [13] A. Eyer, H. Leiste and R. Nitsche, in: *Material Sciences under Microgravity*, ESA SP-222 (ESA, Paris, 1984) pp. 173–181.
- [14] J.F. Padday, in: *Material Sciences under Microgravity*, ESA SP-222 (ESA, Paris, 1984) pp. 9–14.
- [15] I. Martínez and A. Eyer, *J. Crystal Growth* 75 (1986) 535.